Characterization of a Novel MAP4K4-SASH1 Kinase Cascade Regulating Breast Cancer Tumorigenesis and Metastasis

Yadong Li
Guizhou Medical University
Daoqiu Wu
The Affiliated Hospital of Guizhou Medical University
Jing Hou
Guizhou Provincial People's Hospital
Jing Zhang
The Affiliated Hospital of Guizhou Medical University
Xing Zeng
Chongqing Medical University
Lian Chen
Guizhou Medical University
Xin Wan
Guizhou Medical University
Zhixiong Wu
Guizhou medical university
Jinyun Wang
Guizhou Medical University
Ke Wang
Yongchuan Hospital of Chongqing
Dan Yang
The Affiliated Hospital of Guizhou Medical University
Hongyu Chen
Guizhou Medical University
Zexi Xu
Guizhou medical university
Lei Jia
Guizhou Medical University
Qianfan Liu
Guizhou medical university
Zhongshu Kuang

Fudan university
Geli Jiang
Chongqing Cancer Hospital
Hui Zhang
Chongqing Zhongshan Hospital
Jie Luo
Chongqing Cancer Hospital
Wei Li
Chongqing Cancer Hospital
Xue Zou
The Affiliated Hospital of Guizhou Medical University
Xiaohua Zeng
Chongqing Cancer Hospital
Ding'an Zhou (**460318918@qq.com**)
Guizhou Medical University https://orcid.org/0000-0002-6614-9321

Research

Keywords: SASH1, MAP4K4, Tumorigenesis, Metastasis, Hormone-dependent breast cancers

Posted Date: November 5th, 2020

DOI: https://doi.org/10.21203/rs.3.rs-101160/v1

Abstract

Background: The SAM and SH3 domain containing protein 1(SASH1) was previously described as a candidate tumor-suppressor gene in breast cancer and colon cancer to mediate tumor metastasis and tumor growth. However the underlying mechanisms by which SASH1 implements breast cancer tumorigenesis and the question why SASH1 is downregulated in most solid cancers remain unexplored.

Methods: The expression and clinical relevance of SASH1 and mitogen-activated protein kinase kinase kinase kinase 4 (MAP4K4) were analyzed by immunohistochemistry(IHC). The bindings of SASH1 and MAP4K4 were investigated by pull down assay, nano-flow LC-MS/MS , immunoprecipitation- western blot(IP-WB) and immunofluorescence(IF). The knockdown of SASH1- and/or MAP4K4-induced cell proliferation, apoptosis, migration and invasion were investigated by flow cytometry and transwell assays. The cell proliferation and apoptosis treated by GNE-495 were assessed by flow cytometry. The *in vitro* regulation relationship between SASH1 and MAP4K4 were identified by in vitro kinase assay. The functional effects of the silencing of SASH1 and/or MAP4K4 on tumorigenesis and metastasis of T47D cells-xenograft tumors were assessed by HE staining and IHC .

Results: SASH1 and MAP4K4 was significantly downregulated in hormone- dependent subtypes of breast cancers and SASH1 was significantly correlated with MAP4K4 in hormone-dependent subtypes. SASH1 is identified to be a novel serine/threonine protein kinase that binds to MAP4K4, and is phosphorylated by MAP4K4. SASH1 and MAP4K4 synergistically regulate cell proliferation migration and invasion of hormone-dependent breast cancer cells and mediate liver and lung metastasis of T47D cells-xenograft tumors.Ser801 in MAP4K4 might be the serine site for MAP4K4 to phosphorylate SASH1. GNE-495 a MAP4K4-specific inhibitors by upregulating the expression of MAP4K4 and SASH1 might be a potential reagent in treating hormone-dependent breast cancers.

Conclusion: Our findings characterize a novel MAP4K4-SASH1 kinase cascade to mediate the tumorigenesis and metastasis of breast cancer, which can be of targeted intervention by GNE-495.

Background

SASH1 was originally identified as a candidate tumor-suppressor gene in breast cancer and colon cancer, regulating tumorigenesis of breast and other solid cancers and the adhesive and migratory behavior of cancer cells in tumor formation[1, 2]. A growing number of reports have confirmed the tumor suppressor roles of SASH1 in breast and other solid cancers[3–8]. Treatment of breast cancer cells treated with chloropyramine results in higher SASH1 protein levels [9]. SASH1 was recently suggested to be potential therapeutic target for cancer [10]. SASH1 was confirmed to bind to 14-3-3 proteins and phospho-Ser90 of SASH1 provides the 14-3-3-binding sites to promote SASH1 phosphorylation by phosphatidylinositol 3-kinase and MAPK/p90RSK signaling[11]. And the most recent study has indicated that SASH1 was phosphorylated by LATS1 [12].

MAP4K4, is also known as a hepatocyte progenitor kinase-like/germinal center kinase-like kinase (HGK).HGK is a member of the human STE20/ mitogen-activated protein kinase kinase kinase kinase family of serine/threonine kinases and is the ortholog of mouse NIK (Nck-interacting kinase). Strikingly increasing rates of invasion and morphogenesis are induced by enhanced HGK kinase activity through overexpression[13]. MAP4K4 overexpresses in many types of human cancer [14–16]. MAP4K4 is commonly overexpressed in TNBC(triple negative breast cancer)- breast tumor-initiating cells(BTICs) and suggested to be a common regulator in TNBC [17]. The present study indicates that SASH1 is identified to be a novel protein kinase interacts with MAP4K4. MAP4K4 and SASH1 coordinately mediate tumorigenesis and metastasis of breast cancer in hormone-dependent breast cancer cell lines and xenograft tumors. SASH1 is phosphorylated and regulated by MAP4K4, which forms a novel MAP4K4-SASH1 phosphokinase cascade and this cascade can be inhibited by GNE-495 .

Materials And Methods

Collection of breast cancer tissues and human breast carcinoma tissue arrays.

Fresh primary breast cancer tissues from breast carcinoma patients undergoing resection and normal tissues were collected between July 2015 and May 2020 at the Chongqing Cancer Hospital. A set of human breast cancer tissue arrays and a set of matched adjacent tissue arrays of human breast cancer were provided by Shanghai Biochip(Shanghai, China).

Antibodies, cell lines, recombinant DNA or shRNA and siRNAs, and primers for gene cloning and site-directed mutagenesis and siRNA construction.

The detailed information on chemical reagents, antibodies, cell lines, BALB/c-nude mice, recombinant DNA or shRNA and siRNAs, and primers for gene cloning, shRNA silencing of lentivirus, site-directed mutagenesis , siRNA construction used in this study is indicated in Table S1.

Gene cloning

SASH1-Pegfp-C3 vectors were constructed as described previously[18]. MAP4K4 cDNA was cloned into Pbabe-Flag-puro and Pegfp-C3 using KpnI and XhoI restriction sites. SASH1 mutant plasmids were constructed as described previously [18]. Full- length cDNA of SASH1 was cloned into the pSec Tag vector using XhoI and HindIII restriction sites to construct His-SASH1- pSec Tag vector.

Cell Culture, RNA Interference (RNAi), Transfection and lentivirus infection.

Human breast cancer cell lines and HEK-293T cells were obtained from the Cell Bank of the Chinese Academy of Sciences (Shanghai China). After passages, cells were transfected recombined vectors. Cells were transfected with two unique and efficient SASH1-shRNA or MAP4K4-shRNA constructs in a GFP vector (Origene) using PEI(prepared by us) according to our previous reports[18, 19]. The sequences used for silencing of *SASH1*-shRNA vector, silencing of *MAP4K4*-shRNA vector, silencing of *MAP4K4*– shRNA lentivirus and silencing of *SASH1*– shRNA lentivirus were shown in Table S1.

Pull down assay, Nano-flow LC-MS/MS and Database search

The Pull down assay, nano-flow LC-MS/MS and the database search were constructed as previously described. The binding partners of SASH1 and the phosphorylation sites on SASH1 in SK-BR-3 cells were identified with nano-LC MS/MS analysis on an HPLC system as previously described [20].

Immunoprecipitation and immunoblotting

The immunoprecipitation-western blot(IP-WB) assays were performed as previously described[18, 19]. Most of western blot were mainly performed as our previous reports [18, 19].The primary antibodies used for western blotting were as listed in Table S1.

Cell cycle and apoptosis assays

Transfected cells were harvested , fixed , stained and analyzed by flow cytometry (Navious, Beckman Coulter) for cell cycle profile determination [21]. Apoptosis was measured by staining with 7AAD/APC. The results were analyzed using Flowjo software (CT, USA).

Transwell migration and Invasion assay

Transwell migration assay and invasion assays were performed as previously described[22].

Immunofluorescence

Immunofluorescence (IF) was performed as previously described by us[20].

In vitro Kinase assay

For the SASH1 kinase assay, HEK-293T cells were transfected with GFP-MAP4K4 and treated with 150 nM GNE-495 for 24hr and MAP4K4 was immunoprecipitated. His-SASH1 was also introduced into HEK-293T cells and at 36hr after transfection, His-SASH1 was immunoprecipitated with His Ab.The purified His-SASH1 was used as the substrate for the immunoprecipitated MAP4K4. The protocol of this study were mainly referred to the previous report[23] and the detailed protocol of In vitro kinase assay was indicated in the Supplementary Materials and Methods .

Immunohistochemical staining and quantification

Tissue sections (5μm) were dehydrated and subjected to peroxidase blocking. of human breast cancer tissues, normal breast tissues, corresponding adjacent tissues and T47D cells-xenograft tumors were immunohistochemically stained with anti-SASH1, anti-MAP4K4, anti-phospho-MAP4K4, anti-Ki67, anti-MMP2 anti-caspase9 and anti-MMP9. Detailed information on these antibodies can be found in Table S2. The IHC analyses results of p53 and the breast cancer patients' information including age, tumor size, tumor location, tumor stage, node status and clinical stage were provided by the manufacturer of the breast cancer tissue arrays. IHC were mainly performed as previously described[18]. The staining

intensity of SASH1, MAP4K4, phospho-MAP4K4, Ki67, MMP2 and MMP9 of the positive cells, and the positive areas' percentage of the positive cells , and total scores of each visual field were calculated as previously described [18].

Site directed mutagenesis

The wild type SASH1-Pegfp-C3 vector was used to construct SASH1- Pegfp-C3 vectors with S90A、S355A , S359A, S814A and S819A mutations by site-directed mutagenesis using the KOD-Plus-Mutagenesis kit(TOYOBO,Janpan). The wild type MAP4K4- Flag-Pcdna 3.1 vector was also used to construct MAP4K4-Pegfp-C3 vectors with S801A,S629A and S631A mutations by site-directed mutagenesis.

Xenograft

Animals were housed and maintained under specific pathogen-free experimental animal center. T47D stable cells containing SASH1-shRNA or/and were suspended in Matrigel (BD)-DMEM (5×10^6) and injected subcutaneously into the right side fossa axillaris of each 5- to 6-week-old female BALB/c nude mice in each group. Tumor volume was calculated and tumor diameter was measured. All mice were sacrificed 3 weeks after observation, and tumor weights were measured.

Statistical analyses

Data are presented as mean ± SD. Pearson's chi-squared Tests was used to analyze the relationship between IHC scores of the relevant proteins and between clinicopathological parameters and expression levels of SASH1 and p53. The statistical significance of differences was assessed using SPSS16.0 software. The densitometry values of protein bands on western blot were analyzed using a homogeneity of variance test and one-way ANOVA was used for multiple comparisons using the least significant difference in SPSS16.0 to generate the required *P*-values. *P*-values of less than 0.05 were considered statistically significant. The cartograms were made and plotted using GraphPad Prism 5 (GraphPad, Inc, CA, USA). Additional methods can be found in the Supplementary Materials and Methods.

Results

SASH1 is down-regulated in four breast cancer subtypes and its expression is associated with the pathological diagnosis index and receptor expression of breast cancer.

To examine the expression of SASH1 in different breast cancer subtypes, 284 carcinoma specimens of four breast cancer subtypes including 92 luminal A, 105 luminal B, 45 HER2 positive and 42 TNBC specimens, and 79 normal breast tissues including tissues of breast fibroadenoma and hyperplasia of mammary glands were collected to compare SASH1 expression in normal breast tissues and breast cancer tissues. Positive SASH1 staining was found in both ductal and lobular epithelial cells. SASH1 expression was observed predominantly in the cytoplasm (Fig. 1A). SASH1 was significantly downregulated in all four subtypes as compared with normal breast tissues(Fig. 1A and Fig. 1B). SASH1

staining of human breast carcinoma tissue arrays indicated that SASH1 was downregulated in four subtypes as compared with the matched breast tissues (Fig. 1C and Fig. 1D). Immunoblot analyses indicated that in 18 benign breast tissues and 18 cancer tissues, SASH was downregulated in different subtypes of breast cancer (Fig. 1G). Statistical analyses based on IHC staining scores of SASH1 and Ki67 in human breast carcinoma tissue arrays suggested that SASH1 expression was significantly related to that of Ki67 in subtypes of luminal and Her2 positive, however, not associated with that of Ki67 in TNBC subtype(Fig. 1E). The relationship between SASH1 expression and p53 expression obtained by the human breast cancer tissue array was assessed by Pearson's chi-squared test. SASH1 expression was significantly related to p53 in subtypes of luminal and Her2 positive, however, not related to Ki67 in TNBC subtype (Fig. 1F). SASH1 downregulation was significantly associated with early tumor stages,early lymph node metastasis, and early clinical stage; however, it was not correlated with tumor size(Table S2). We also analyzed the relationship of SASH1 expression with ER, PR, EGFR, p53 and CK5/6 in human breast carcinoma tissue arrays. Pearson's $\chi 2$ test based their IHC scores and their positive rate indicated that SASH1 expression was inversely correlated with the ER of nucleus and cytoplasm(Fig.S1A and S1B). SASH1 expression was negatively correlated with the nucleic and cytoplasmic PR (Fig.S1C and S1D).However, SASH1 expression was positively correlated with the nucleic HER2 (Fig.S1E). SASH1 expression was positively correlated with the nucleic and cytoplasmic p53 ae well as Ki67(Fig.S1F, Fig.S1G and Fig.S1H).However, SASH1 expression was not correlated with the EGFR of cytoplasm and cytoplasm membrane(Fig.S1I and S1J) and CK5/6(Fig.S1K).

SASH1 is associated with MAP4K4.

To investigate the molecular network in which SASH1 involved, pull down assays and LC-MS/MS spectrometry analysis were performed. Our results indicated that SASH1 may interact with MAP4K4 in stable SK-BR-3 cells. MAP4K4 was shown to have a high possibility to bind to SASH1 (Fig. 2A), and the interacting peptide sequences of SASH1 and MAP4K4 were identified (Fig. 2B). IP-WB analysis further confirmed that endogenous SASH1 was associated with endogenous MAP4K4 (Fig. 2C). We also found exogenous SASH1 binds to endogenous MAP4K4 using IP with anti GFP antibody. As demonstrated in Fig. 2D, exogenous SASH1 was shown to immunoprecipitate with endogenous MAP4K4 in SK-BR-3 cells. We further identified the binding domains of SASH1 to MAP4K4. Deleted SASH1 constructs were created, transfected into HEK-293T cells and immunoprecipitated with anti-GFP antibody. The associated endogenous MAP4K4 were identified by IP-WB. Compared with the binding of full- length SASH1 to endogenous MAP4K4, the N-terminal domain of SASH1 (SASH1-ΔC terminal) was shown to bind to endogenous MAP4K4 (Fig. 2F and Fig. 2G). In addition, we observed co-localization between endogenous SASH1 and endogenous MAP4K4 in T47D and MCF-7 cells (Fig. 2H and Fig. 2I).

SASH1 expression is positively correlated with MAP4K4 expression and downregulation of SASH1 is positively associated with increased phospho-MAP4K4 levels in breast cancer.

Since SASH1 was shown to bind to MAP4K4, the expression of MAP4K4 and the relationship between SASH1 and MAP4K4 levels in breast cancers were investigated. A total of 284 carcinoma specimens of

breast cancer and 79 normal breast tissues including tissues of breast fibroadenoma and hyperplasia of mammary glands were collected to analyze the relationship between SASH1 and MAP4K4 in normal breast tissues and breast cancer tissues. MAP4K4 expression was detected predominantly in the cytoplasm and on the plasma membrane in some cases. In four breast cancer subtypes especially the luminal and HER2 positive subtypes as well as normal breast tissues,SASH1 was significantly associated with MAP4K4. Statistical analysis of IHC scores of SASH1 and MAP4K4 revealed that SASH1 was obviously correlated with MAP4K4 in normal breast tissues (Fig. 3A). In the subtypes of luminal A, luminal B and HER2 positive (Fig. 3B, Fig. 3C and Fig. 3D) SASH1 was obviously correlated with MAP4K4. However,SASH1 was also correlated with MAP4K4 in TNBC subtype (Fig. 3E). Although *MAP4K4* mRNA levels in TNBC cells were higher than in non-TNBC cells，MAP4K4 protein levels were not higher than in non-TNBC cells[17]. Statistical analysis of IHC scores indicated that MAP4K4 expression of 284 breast carcinoma specimens was lower than that of 79 normal breast tissues(Fig. 3G and Fig. 3H). Western blot analysis indicated that in 10 pairs of breast cancer tissues and normal breast tissues, in most breast cancer specimens， downregulation of MAP4K4 was accompanied by decreased SASH1 levels (Fig. 3I). In addition, statistical analysis of IHC scores indicated that SASH1 expression was correlated with phospho-MAP4K4 levels in 75 breast cancer tissues (Fig. 3J). These IHC results revealed that in breast cancer tissues， SASH1 expression is correlated with MAP4K4 expression，and increased phospho-MAP4K4 levels are correlated with SASH1 expression.

MAP4K4 and SASH1 co-regulate proliferation, migration and invasion of luminal subtype and HER2 positive subtype cell lines.

Since SASH1 expression is correlated with MAP4K4 expression in the luminal subtype and the HER2 positive subtype, we further assessed their roles in breast cancer tumorigenesis. We first performed loss-of-function studies using lentiviruses expressing two distinct short hairpin RNAs (shRNAs) against *SASH1* to knockdown SASH1 in two luminal subtype cell lines, T47D and MCF-7. The distribution of G1, G2/M, and S-phases of T47D cells were determined by flow cytometry and SASH1 silencing increased the proportion of S-phase cells and decreased the proportion of G1-phase cells(Fig. 4A). Moreover, flow cytometry analyses indicated that SASH1 knockdown induced less proportion of early apoptotic cells(Fig. 4B). We further analyzed the effects of loss-of-function of *SASH1* on the migration and invasion of T47D cells. Transwell assays revealed that migration and invasion of T47D cells were induced by *SASH1* deletion (Fig. 4C and Fig. 4D). Flow cytometry analyses suggested that *MAP4K4* knockdown increased the proportion of G2/M-phase cells and induced more proportion of early apoptotic cells (Fig. 4F and Fig. 4G). Transwell assays indicated that *MAP4K4* knockdown inhibited the cell numbers of migrating and invasive cells when T47D cells were silenced by *MAP4K4*-shRNA lentivirus (Fig. 4H and Fig. 4I). We further co-silenced *SASH1* and *MAP4K4* and evaluated the effects of co-silencing of *SASH1* and *MAP4K4* on cell growth， migration and invasion of T47D. The cell cycle profiles indicated that although *MAP4K4* deletion did not significantly change the inducement of *SASH1* silencing to the increased proportion of S-phase cells，MAP4K4 knockdown could significantly increase the proportion of early apoptotic cells(Fig. 4K and Fig. 4L). Meanwhile, MAP4K4 deletion significantly abolished the inducement of SASH1 silencing to enhance the migration and invasion ability of T47D cells (Fig. 4N and

Fig. 4O). In the other luminal subtype cell line, MCF-7, *SASH1* silencing also increased the proportion of S-phase cells and decreased the proportion of G1-phase cells(Fig.S2A)，and *SASH1* knockdown also induced decreased proportion of apoptotic cells of MCF-7 cells(Fig.S2B). The cell cycle profiles indicated that *MAP4K4* deletion decreased the proportion of S-phase cells (Fig.S2C) and induced increased proportion of apoptotic cells of MCF-7 cells (Fig.S2D). Similarly, in the co-silenced MCF-7 cells, although *MAP4K4* deletion did not significantly change the inducement of *SASH1* silencing to the increased proportion of S-phase cells, *MAP4K4* silencing significantly increased the proportion of early apoptotic cells (Fig.S2E and Fig.S2F).

In the $HER2^+$ subtype cell line,SK-BR-3 cells, *SASH1* was silenced by two pairs of specific *SASH*1-shRNA, and the distribution of G1,G2/M， and S-phases was determined by flow cytometry. SASH1 silencing increased the proportion of S-phase cells and decreased the proportion of G2/M-phase cells (Fig. S3A and Fig.S3C). Moreover， flow cytometry analysis revealed after *SASH1* silencing，a significantly smaller proportion of early apoptotic cells was observed (Fig. S3B and Fig.S3C). Specific *MAP4K4*-shRNAs were also introduced into SK-BR-3 cells; cell cycle analyses showed that the interference with MAP4K4 expression increased proportion of G2/M-phase cells and decreased the proportion of S-phase cells，which suggested MAP4K4 silencing induced cell cycle arrest in the G2/M-phase (Fig. S3D and S3F). Flow cytometry analyses also demonstrated that a significantly higher proportion of early apoptotic cells were observed after MAP4K4 silencing (Fig. S3E and S3F). Co-silencing of *SASH1* and *MAP4K4* induced cell cycle arrest in the G2-phase and a decrease in the proportion of S-phase cells, which suggested that the increase in S-phase cells upon *SASH1* silencing in SK-BR-3 cells was prevented by *MAP4K4* silencing，and MAP4K4 silencing resulted in G2/M-phase cell cycle arrest(Fig. S3G and S3I). In addition, increased proportion of apoptotic cells was induced by co-silencing of *SASH1* and *MAP4K4* (Fig. S3H and S3I).

Loss-of-function of MAP4K4 impairs the ability of SASH1 silencing to promote cell proliferation and metastasis of the xenograft of ER + breast cancer cells.

We further identified the effects of loss-of-function of SASH1 and/or MAP4K4 on T47D cells xenograft. T47D cells with stable SASH1 knockdown, *MAP4K4* knockdown and co-silencing of *SASH1* and *MAP4K4* were cultured and injected subcutaneously into the left side fossa axillaris of BALB/c female nude mice. MAP4K4 deletion inhibited the tumor growth including tumor size and tumor weight in the xenograft mouse model with MAP4K4 silencing and co-silencing of *SASH1* and *MAP4K4* (Fig. 5A, 5B, 5C and 5D). We also evaluated the influence of silencing of *SASH1* and/or *MAP4K4* on the metastasis of T47D cells xenograft. *SASH1* silencing induced more liver metastatic lesions in the xenograft mouse models with *SASH1* silencing compared with those in the xenograft mouse models with negative control(NC), *MAP4K4* silencing and co-silencing of *SASH1* and *MAP4K4*(Fig. 5E). We further identified the micro-metastases of liver using H&E staining by counting the number of metastatic lesions in the liver tissues of each mouse. H&E staining revealed that knockdown of SASH1 substantially enhanced the invasiveness of the T47D derived xenograft tumors(Fig. 5F and Fig. 5G). *MAP4K4* deletion did not significantly reduce the number of liver metastatic lesions, however, *MAP4K4* deletion could significantly reduce the increased numbers of

liver metastatic lesions induced by SASH1 silencing (Fig. 5F and Fig. 5G). Furthermore, pulmonary micro-metastases were examined by H&E staining and the total number of pulmonary metastatic lesions in each mouse were counted. The results showed that more and larger pulmonary micro-metastases were detected in the mice model with *SASH1*-depleted T47D cells than in the control mice. Although *MAP4K4* deletion did not significantly reduce the number of pulmonary metastatic lesions, *MAP4K4* deletion could significantly reduce the increased numbers of liver metastatic lesions induced by *SASH1* silencing (Fig. 5H and Fig. 5I). We further evaluated the influence of *SASH1* and/or *MAP4K4* silencing on the molecular index of proliferation and metastasis. *MAP4K4* knockdown *in vivo* reversed the SASH1 downregulation induced by *SASH1* silencing in the T47D cells-xenograft tumors co-silenced with *SASH1* and *MAP4K4*-shRNA lentivirus, and *MAP4K4* silencing upregulated SASH1 expression in the xenograft tumors silenced with MAP4K4-shRNA lentivirus(Fig. 6A). *SASH1* silencing induced upregulated expression of Ki67 and increased numbers of Ki67-positive cells in the xenograft tumors silenced with *SASH1*- shRNA lentivirus. *MAP4K4* knockdown abolished the inducement of Ki67 expression and increased Ki67-positive cells by *SASH1* silencing in the xenograft tumors co-silenced with the lentivirus of *SASH1*-shRNA and *MAP4K4*-shRNA(Fig. 6C). However ,*SASH1* silencing did not change the expression of caspase 9、MMP2 and MMP9 in the T47D cells-xenograft tumors silenced with *SASH1*-shRNA lentivirus(data not shown).

SASH1 acts as a protein kinase and is phosphorylated by MAP4K4.

To identify the reason that SASH1 is downregulated in most of tumors and tumor cells, The phosphorylation modification sites on SASH1 were identified by LC- MS/MS analysis. Ser355, Ser359, Ser914 and Ser918 are potential phosphorylation modification sites (Fig. S4A and S4B). Actually, previous report has suggested that Ser90 of SASH1 is the phosphorylation modification site of SASH1[11]. We further investigated whether SASH1 is phosphorylated by MAP4K4 and which serine sites of SASH1 were the key phosphorylation sites. SASH1 was identified to be a very unstable protein and exogenous SASH1 and endogenous MAP4K4 began to degrade after cycloheximide (CHX) treatment (Fig. 7A). Decreased exogenous SASH1 expression and a backward shift of the SASH1 protein bands in GFP-SASH1-transfected SK-BR-3 cells were observed after treatment with the serine/threonine phosphatase inhibitor calyculin A (Fig. 7B), which indicates that SASH1 is a novel serine protein kinase. Calyculin A-induced SASH1 degradation and calyculin A-induced MAP4K4 degradation were blocked upon the proteasome inhibitor MG132(Fig. 7C), which indicated that MAP4K4 and SASH1 are both phosphorylated. GNE-495 is a potent and selective MAP4K4 inhibitor and inhibit MAP4K4 function *in vivo*[24]. To identify the inhibitory effects of GNE-495 to MAP4K4 in breast cancer cells and investigate whether GNE-495 can block the phosphorylation of MAP4K4. SK-BR-3 cells were treated with different concentrations of GNE-495 and western blot showed that 100 nM GNE-495 could efficiently inhibit phospho-MAP4K4 expression and upregulated the protein levels of endogenous MAP4K4 and SASH1 (Fig. 7D). Treatment with GNE-495 not only increased expression of SASH1 and MAP4K4 but also enhanced bindings of SASH1 to MAP4K4 (Fig. 7E). The calyculin A- induced decreases in phosphorylation of exogenous SASH1 and exogenous MAP4K4 were abolished by GNE-495 treatment (Fig. 7F). The SASH1 phosphorylation sites Ser355, Ser359, Ser914, and Ser918 are highly conserved, as

analyzed by Clustal X2 software(Fig. 7G). Immunoblot analysis indicated that Ser359 and Ser914 are the key phosphorylation sites of SASH1 because the mutations of S359A and S914A caused little changes in SASH1 expression after GNE-495 treatment as compared with wild type SASH1 and other SASH1 mutants. Especially S914A caused a forward shift of the SASH1 protein band (Fig. 7H, 7I and 7J). IP-WB revealed that these two mutations increased binding of SASH1 to MAP4K4 and GNE-495 not only promoted the binding of wild type SASH1 but also of mutated SASH1 to MAP4K4 (Fig. 7K).

GNE-495 may reverse MAP4K4-mediated phosphorylation of SASH1 and upregulates both protein levels of MAP4K4 and SASH1.

MAP4K4 over-expression downregulated endogenous SASH1 expression in hormone- dependent breast cancer cell lines,SK-BR-3 and MCF-7 cells(Fig. 8A). Exogenous SASH1 was upregulated upon *MAP4K4* knockdown (Fig. 8B). Bioinformatics analysis by Clustal X2 software indicated that Ser629, Ser631 and Ser801 of MAP4K4 are highly conserved phosphorylation sites (Fig. 8C). Western blot analysis suggested that the S801A mutation of MAP4K4 induced a forward shift of the MAP4K4 protein bands and unlike exogenous SASH1 was upregulated after the phosphorylation inhibition of GNE-495 treatment to MAP4K4S801A mutation of MAP4K4 could not upregulate or attenuated the expression of exogenous SASH1 in SK-BR-3 and HEK-293T cells (Fig. 8D and Fig. 8E). In addition, the S801A mutation of MAP4K4 not only induced a forward shift of MAP4K4 main bands but also caused the appearance of multiple SASH1protein (Fig. 8D and Fig. 8E). Similarly, the S801A mutation in MAP4K4 attenuated the GNE-495-induced-endogenous SASH1 upregulation (Fig. 8F and Fig. 8G). Further IP-WB analyses revealed that S801A mutation in MAP4K4 attenuated the bindings of MAP4K4 to SASH1 compared with wild type MAP4K4 (Fig. 6H) *in vivo*. We performed *in vitro* kinase assay to identify the phosphorylation of MAP4K4 to SASH1. GNE-495 not only upregulates the expression of wild type MAP4K4 but also that of S801A-MAP4K4. Being similar to the *in vivo* results indicated above, GNE-495 promoted the bindings of wild type MAP4K4 to his-SASH1, however, attenuated the association S801A- MAP4K4 tohis-SASH1 *in vitro* (Fig. 6I). In addition GNE-495 treatment caused a significant apoptosis in hormone-dependent breast cancer cells and MAP4K4 deletion can impair the induced apoptosis by GNE-495(supplementary Fig.S5).

Discussion

Although growing evidence suggests that SASH1 is a tumor suppressor in breast cancer[25] [2, 26, 27], the mechanism by which SASH1 regulates tumor behaviors including tumorigenesis,adhesion and migration on cancer cells in cancer development and progression remain completely unclear[25]. Recent evidence reveal that SASH1 might be phosphorylated by LATS1 and LATS2[12, 28]. In this study, we firstly reveal that SASH1 acting as a novel protein kinase is phosphorylated by MAP4K4, to constitute a novel MAP4K4-SASH1 phosphokinase cascade to mediate tumorigenesis and metastasis of hormone-dependent breast cancer. Taken the previous findings into consideration, a MAP4K4-LATS1/LATS2-SASH1 signal cascade may mediate the tumorigenesis and metastasis of breast cancer. FunctionallyMAP4K4 existence is necessary to SASH1. *MAP4K4* deletion will abolish the SASH1-induced tumorigenesis and metastases *in vitro* and *in vivo*. Importantly, GNE-495 specifically inhibits MAP4K4

phosphorylation and not only upregulate MAP4K4 protein level but also that of SASH1. GNE-495 by preventing the phosphorylation of the MAP4K4-SASH1 phosphorylation cascade might be a novel effective inhibitor, inhibits tumorigenesis of hormone-dependent breast cancer. Therefore, our findings firstly reveal a novel kinase cascade that can be targeted by small molecular compounds to treat hormone-dependent breast cancers. Previous reports have revealed that Ser90 in SASH1 serves as the 14-3-3-binding sites to induce SASH1 phosphorylation by phosphatidylinositol 3-kinase and MAPK/p90RSK signaling [17] and Ser407 in SASH1 is the key serine site for LATS1-mediated phosphorylation of SASH1[12]. Ser 914 in SASH1 in the present study is identified to be another serine site for MAP4K4-mediated phosphorylation of SASH1.

The serine/threonine kinase MAP4K4 is a member of the Ste20p (sterile 20 protein) family and increasing evidence suggests that MAP4K4 also plays an important role in cancer[29]. Current evidence suggests that MAP4K4 potentially serves as a negative prognostic indicator in patients with colorectal cancer[30], hepatocellular carcinoma [31], pancreatic ductal adenocarcinoma [32], lung adenocarcinoma [33] and prostate cancer [34]. MAP4K2, MAP4K4 and MAPK1 have been identified as kinases that mediate paracrine growth signaling in ER-negative breast cancers[35]. In this study, our findings indicate that in breast cancer, especially the luminal A and TNBC subtypes, MAP4K4 is downregulated compared to normal breast tissues. Generally, cell apoptosis[31, 36–39], cell cycle arrest[31, 38, 39], and migration and invasion [40] [38, 39, 41, 42] are induced by MAP4K4 downregulation in cancer cells. In this study, MAP4K4 silencing in induces cell cycle arrest, apoptosis and block migration and invasion in hormone-dependent breast cancer cell lines and T47D cells-xenograft tumors. MAP4K4, in a kinase activity-dependent manner, positively regulate cell transformation and invasion and negatively regulates cell spreading and adhesion[13]. MAP4K4 physically interacts with both LATS1 and LATS2 and phosphorylates LATS1 and LATS2 [28] and SASH1 was phosphorylated by LAST1[12]. Our findings indicated that MAP4K4 physically interacts with SASH1 and MAP4K4 may indirectly phosphorylate SASH1. However, MAP4K4 deletion will impair the inducement of loss-of-function of SASH1 to tumorigenesis,adhesion and migration of hormone-dependent breast cancer in breast cancer cell lines and xenograft tumors. So functionally, the existence of MAP4K4 is necessary to SASH1 and there may be a balance of expression levels between MAP4K4 and SASH1. Ser801 in MAP4K4 are identified might to be the key sites for MAP4K4-mediated phosphorylation of SASH1.

Given the diverse roles of MAP4K4 in many cell processes, the therapeutic potential of MAP4K4 inhibition will be appealing and it's worth identifying the MAP4K4 inhibitor that would function in vivo[24]. Some of the inhibitors show promise in treating pathological angiogenesis in mice[24, 43]. MAP4K4 may represent a novel actionable cancer therapeutic target. Whether these inhibitors possess potent antitumor properties remains to be determined[29]. In this study, GNE-495 not only inhibits phospho-MAP4K4 protein level and upregulates MAP4K4 but also increases SASH1 protein level, which eventually induce the apoptosis of hormone-dependent breast cancer cells.

Conclusion

Therefore, our findings firstly reveal a novel SASH1-MAP4K4 phosphoprotein kinase cascade that may serve as a therapeutic intervention to treat hormone-dependent breast cancers.

Abbreviations

BTICs: Breast tumor-initiating cells; CHX: Cycloheximide; DMEM: Dulbecco's modified eagle medium; HER2: Human epidermal growth factor receptor 2;

HGK: Hepatocyte progenitor kinase-like/germinal center kinase-like kinase; IF: Immunofluorescence; IP-WB: Immunoprecipitation- western blot; LATS1: Large tumor suppressor kinase 1; LATS2: Large tumor suppressor kinase 2; MAPK : Mitogen-activated protein kinase kinase; MAP4K4: Mitogen-activated protein kinase kinase kinase kinase 4; NIK: Nck-interacting kinase; SASH1: SAM and SH3 domain containing protein 1; TNBC: Triple negative breast cancer.

Declarations

Acknowledgements

Not applicable.

Authors' Contributions

Conception and design: D.A. Zhou, X.H. Zeng; Development of methodology: D.A. Zhou, Y.D. Li; Acquisition of data (provided animals, acquired and managed patients, provided facilities, etc.): Y.D. Li D.Q. Wu, J. Hou X. Zeng, L. Chen, X. Wan, J. Zhang, Z.X Wu K. Wang, Y. Wang , D. Yang, H.Y Chen Z.X. Xu L. Jia Q.F. Liu, J. Wang Z.S Kuang G.L Jiang, H. Zhang, J. Luo, W. Li, X. Zou, X.H Zeng; Analysis and interpretation of data (e.g., statistical analysis, biostatistics,

computational analysis): D.A. Zhou, Y.D. Li; Writing, review, and/or revision of the manuscript: D.A. Zhou, X.H. Zeng; Administrative, technical, or material support (i.e., reporting or organizing data, constructing databases): D.A. Zhou, X.H. Zeng, J. Hou.

Funding

This work was supported by the National Natural Science Foundation Project of China (grant numbers: 31860319 and 32060165 to D.A. Zhou and grant number: 81702640 and 81660439 to J. Hou) and the Guizhou Provincial Natural Science Foundation (grant numbers: Qian Ke He Zhicheng [2020]4Y125 to D.A. Zhou) , the Science and technology bureau of Chongqing (grant number:cstc2018jxjl130044) to X.H. Zeng) , and the Guizhou Province Education Department Youth Science and Technology Talent Growth Project (No. [2016]143) to X.Zou).

Availability of data and materials

All data generated or analyzed during this study are included in this published article.

Ethics approval and consent to participate

This study was approved by the Institutional Ethics Committee of the Affiliated Hospital of Guizhou Medical University and Chongqing Cancer Hospital (authorization number: 2018 lunshen No.059).

Consent for publication

Informed consent was obtained from all individual participants included in

the study.

Competing interests

The authors declare that they have no conflicts of interest.

Author details

[1]Clinical Research Center, the Affiliated Hospital of Guizhou Medical University, Guiyang, Guizhou, 550004,P.R. China. [2] Clinical College, Guizhou Medical University, Guiyang, Guizhou, 550004, P.R. China. [3] School of Clinical Laboratory Science, Guizhou Medical University, Guiyang,Guizhou, 550004, P.R. China. [4] Breast Cancer Surgery Department, Guizhou Provincial People's Hospital. Guiyang,Guizhou, 550001, P.R. China. [5] The Fifth Clinical College, Chongqing Medical University, Chongqing, 400010, China. [6]School of Biology and Engineering, Guizhou Medical University, Guiyang,Guizhou, 550004, P.R. China. [7] Department of Laboratory Medicine, Yongchuan District Hospital, Chongqing, 402160, P.R. China. [8] Zhongshan Hospital, Fudan University, Shanghai, 200032, China. [9] Chongqing University Cancer Hosiptal & ChongqingCancer Institute & Chongqing cancer hospital, Chongqing, 400030, P.R. China. # These authors contribute equally to these work.

References

1 Rimkus C, Martini M, Friederichs J, Rosenberg R, Doll D, Siewert JR *et al*. Prognostic significance of downregulated expression of the candidate tumour suppressor gene SASH1 in colon cancer. *Br J Cancer* (Comparative Study Research Support, Non-U.S. Gov't) 2006; 95: 1419-1423.

2 Zeller C HB, Seitz S, Prokoph H, Burkhard-Goettges E, Fischer J, Jandrig B, Schwarz LE, Rosenthal A, Scherneck S. SASH1: a candidate tumor suppressor gene on chromosome 6q24.3 is downregulated in breast cancer. *Oncogene* 2003; 22: 2972-2983.

3 Burgess JT, Bolderson E, Adams MN, Baird AM, Zhang SD, Gately KA *et al*. Activation and cleavage of SASH1 by caspase-3 mediates an apoptotic response. *Cell Death Dis* 2016; 7: e2469.

4 Joshua T. Burgess EB, Jodi M. Saunus, Shu-Dong Zhang, Lynne E. Reid, Anne Marie McNicol, Sunil R. Lakhani, Katharine Cuff, Kerry Richard, Derek J. Richard1,9, Kenneth J. O'Byrne. SASH1 mediates sensitivity of breast cancer cells to chloropyramine and is associated with prognosis in breast cancer. *Oncotarget* 2016; 7: 72807-72818.

5 Gong X, Wu J, Wu J, Liu J, Gu H, Shen H. Correlation of SASH1 expression and ultrasonographic features in breast cancer. *Onco Targets Ther* 2017; 10: 271-276.

6 Stubblefield K CJ, Nguyen T, Chen CJ, Shively JE. The adaptor SASH1 acts through NOTCH1 and its inhibitor DLK1 in a 3D model of lumenogenesis involving CEACAM1. *Exp Cell Res* 2017; 359: 384–393.

7 Sun C ZZ, He P, Zhou Y, Xie X. Involvement of PI3K/Akt pathway in the inhibition of hepatocarcinoma cell invasion and metastasis induced by SASH1 through downregulating Shh-Gli1 signaling. *Int J Biochem Cell Biol* 2017; 89: 95–100.

8 Citron F, Armenia J, Franchin G, Polesel J, Talamini R, D'Andrea S *et al*. An Integrated Approach Identifies Mediators of Local Recurrence in Head and Neck Squamous Carcinoma. *Clin Cancer Res* 2017; 23: 3769-3780.

9 Joshua T Burgess EB, Jodi M Saunus , Shu-Dong Zhang , Lynne E Reid , Anne Marie McNicol , Sunil R Lakhani, Katharine Cuff , Kerry Richard , Derek J Richard , Kenneth J O'Byrne. SASH1 Mediates Sensitivity of Breast Cancer Cells to Chloropyramine and Is Associated With Prognosis in Breast Cancer. *Oncotarget,* 2016; 7: 72807-72818.

10 QianqianWang H. SASH1, a potential therapeutic target for cancer. *Human Pathology* 2018; 80: 247.

11 Dubois F, Vandermoere F, Gernez A, Murphy J, Toth R, Chen S *et al*. Differential 14-3-3 affinity capture reveals new downstream targets of phosphatidylinositol 3-kinase signaling. *Mol Cell Proteomics* 2009; 8: 2487-2499.

12 Ke Jiang PL, Huizhe Xu 1 , Dapeng Liang 1 , Kun Fang 1 , Sha Du 1 , Wei Cheng 1 , Leiguang Ye 4 , Tong Liu 5 , Xiaohong Zhang 1 , Peng Gong 2 3 , Shujuan Shao 6 , Yifei Wang 7 , Songshu Meng. SASH1 suppresses triple-negative breast cancer cell invasion through YAP-ARHGAP42-actin axis. *Oncogene* 2020; 39: 5015-5030.

13 Jocelyn H. Wright XW, Gerard Manning, Brandon J. LaMere, Phuong Le, Shirley Zhu, Deepak Khatry, Peter M. Flanagan, Sharon D. Buckley, David B. Whyte, Anthony R. Howlett, James R. Bischoff, Kenneth E. Lipson, and Bahija Jallal. The STE20 Kinase HGK Is Broadly Expressed in Human Tumor Cells and Can Modulate Cellular Transformation, Invasion, and Adhesion. *MOLECULAR AND CELLULAR BIOLOGY,* 2003; 23: 2068-2082.

14 Collins CS, Hong, J., Sapinoso, L., Zhou, Y., Liu, Z., Micklash, K., Schultz, P. G., and Hampton, G. M. A small interfering RNA screen for modulators of tumor cell motility identifies MAP4K4 as a promigratory

kinase. *Proc Natl Acad Sci U S A* 2006; 103: 3775-3780.

15 Liang JJ WH, Rashid A, Tan TH, Hwang RF, Hamilton SR, Abbruzzese JL, Evans DB, Wang H. Expression of MAP4K4 is associated with worse prognosis in patients with stage II pancreatic ductal adenocarcinoma. *Clin Cancer Res* 2008; 14: 7043-7049.

16 An-Wen Liu JC, Xiang-Li Zhao, Ting-Hui Jiang, Tian-Feng He, Hua-Qun Fu,Ming-Hua Zhu, and Shu-Hui Zhang. ShRNA-Targeted MAP4K4 Inhibits Hepatocellular Carcinoma Growth. *Clin Cancer Research* 2011; 17: 710-720.

17 Yi-Hsin Hsu1 JY. Definition of PKC-a, CDK6, and MET as Therapeutic Targets in Triple-Negative Breast Cancer. *Cancer research* 2014; 74: 4822-4835.

18 Ding'an Zhou ZW, Zhongshu Kuang , Huangchao Luo , Jiangshu Ma , Xing Zeng ,Ke Wang , Beizhong Liu , Fang Gong , Jing Wang , Shanchuan Lei , Dongsheng Wang , Jiawei Zeng , Teng Wang , Yong He , Yongqiang Yuan , Hongying Dai , Lin He , Qinghe Xing. A novel P53/POMC/Gαs/SASH1 autoregulatory feedback loop activates mutated SASH1 to cause pathologic hyperpigmentation. *J Cell Mol Med* 2017; 21: 802-815.

19 Zhou D, Kuang Z, Zeng X, Wang K, Ma J, Luo H *et al*. p53 regulates ERK1/2/CREB cascade via a novel SASH1/MAP2K2 crosstalk to induce hyperpigmentation. *J Cell Mol Med* 2017; 21: 2465-2480.

20 Zhou D, Wei Z, Deng S, Wang T, Zai M, Wang H *et al*. SASH1 regulates melanocyte transepithelial migration through a novel Galphas-SASH1-IQGAP1-E-Cadherin dependent pathway. *Cell Signal* 2013; 25: 1526-1538.

21 Yang D LL, Liu H, Wu L, Luo Z, Li H et al. Induction of autophagy and senescence by knockdown of ROC1 E3 ubiquitin ligase to suppress the growth of liver cancer cells. . *Cell Death Differ* 2013; 20: 235-247.

22 Lihui Li Mingsong W, Guangyang Yu, Ping Chen, Hui Li, Dongping Wei, Ji Zhu, Li Xie, Huixun Jia, Jieyi Shi, Chunjie Li, Wantong Yao, Yanchun Wang, Qiang Gao, Lak Shin Jeong, Hyuk Woo Lee, Jinha Yu, Fengqing Hu, Ju Mei, Ping Wang, Yiwei Chu, Hui Qi, Meng Yang, Ziming Dong, Yi Sun, Robert M. Hoffman, Lijun Jia. Overactivated Neddylation Pathway as a Therapeutic Target in Lung Cancer. *J Natl Cancer Inst* 2014; 106: dju083.

23 Zhou X WS, Wang Z, Feng X, Liu P, Lv XB, Li F, Yu FX, Sun Y, Yuan H, Zhu H, Xiong Y, Lei QY, Guan KL. Estrogen regulates Hippo signaling via GPER in breast cancer. *J Clin Invest* 2015; 125: 2123-2135.

24 Ndubaku CO CT, Chen H, Boggs JW, Drobnick J, Harris SF et al. Structure-Based Design of GNE-495, a Potent and Selective MAP4K4 Inhibitor with Efficacy in Retinal Angiogenesis. . *ACS medicinal chemistry letters* 2015; 6: 913-918.

25 Martini M, Gnann A, Scheikl D, Holzmann B, Janssen KP. The candidate tumor suppressor SASH1 interacts with the actin cytoskeleton and stimulates cell-matrix adhesion. *Int J Biochem Cell Biol* (Research Support, Non-U.S. Gov't) 2011; 43: 1630-1640.

26 Sheyu L, Hui L, Junyu Z, Jiawei X, Honglian W, Qing S *et al*. Promoter methylation assay of SASH1 gene in breast cancer. *J BUON* 2013; 18: 891-898.

27 Aravind Kumar M, Singh V, Naushad SM, Shanker U, Lakshmi Narasu M. Microarray-based SNP genotyping to identify genetic risk factors of triple-negative breast cancer (TNBC) in South Indian population. *Mol Cell Biochem* 2018; 442: 1-10.

28 Meng Z, Moroishi T, Mottier-Pavie V, Plouffe SW, Hansen CG, Hong AW *et al*. MAP4K family kinases act in parallel to MST1/2 to activate LATS1/2 in the Hippo pathway. *Nat Commun* 2015; 6: 8357.

29 Xuan Gao CG, Guoxiang Liu , Jing Hu. MAP4K4: an emerging therapeutic target in cancer. *Cell Biosci* 2016; 6: 56.

30 Jun-Mei Hao J-ZC, Hong-Mei Sui, Xue-Qing Si-Ma, Guang-Qiu Li, Chao Liu, Ji-Liang Li, Yan-Qing Ding, Jian-Ming Li. A five-gene signature as a potential predictor of metastasis and survival in colorectal cancer. *J Pathol* 2010; 220: 475–489.

31 Liu AW, Cai J, Zhao XL, Jiang TH, He TF, Fu HQ *et al*. ShRNA-targeted MAP4K4 inhibits hepatocellular carcinoma growth. *Clin Cancer Res* 2011; 17: 710-720.

32 Liang JJ WH, Rashid A, Tan TH, Hwang RF, Hamilton SR, Abbruzzese JL, Evans DB. Expression of MAP4K4 is associated with worse prognosis in patients with stage II pancreatic ductal adenocarcinoma. *Clinical Cancer Research* 2008; 14: 7043–7049.

33 Mei-Hua Qiu Y-MQ, Xiang-Li Zhao, Shou-Mei Wang, Xiao-Jun Feng, Xin-Fang Chen, Shu-Hui Zhang. Expression and prognostic significance of MAP4K4 in lung adenocarcinoma. *Pathol Res Pract* 2012; 208: 541-548.

34 Rizzardi AE, Rosener NK, Koopmeiners JS, Isaksson Vogel R, Metzger GJ, Forster CL *et al*. Evaluation of protein biomarkers of prostate cancer aggressiveness. *BMC Cancer* 2014; 14: 244.

35 Corey Speers AT, Krystal Sexton, Ashley M. Herrick, Carolina Gutierrez, Aedin Culhane, John Quackenbush, Susan Hilsenbeck, Jenny Chang, and Powel Brown. Identification of Novel Kinase Targets for the Treatment of Estrogen Receptor-Negative Breast Cancer. *Clin Cancer Res* 2009; 15: 6327–6340.

36 Ning Yang YW, Lian Hui , Xiaotian Li , Xuejun Jiang. Silencing SOX2 expression by rna interference inhibits proliferation, invasion and metastasis, and induces apoptosis through MAP4K4/JNK signaling pathway in human laryngeal cancer TU212 cells. *J Histochem Cytochem* 2015; 63: 721–733.

37 Si Chen XL, Dan Lu, Yingxi Xu, Wenjun Mou, Lina Wang, Yanan Chen, Yanhua Liu. SOX2 regulates apoptosis through MAP4K4-Survivin signaling pathway in human lung cancer cells *Carcinogenesis* 2014; 35: 613–623.

38 Gang Zhao BW, Yang Liu, Jun-Gang Zhang, Shi-Chang Deng, Qi Qin, Kui Tian, Xiang Li, Shuai Zhu, Yi Niu, Qiong Gong, Chun-You Wang. miRNA-141, downregulated in pancreatic cancer, inhibits cell proliferation and invasion by directly targeting MAP4K4. *Mol Cancer Ther* 2013; 12: 2569-2580.

39 Yuan-Fei Liu G-QQ, Yun-Min Lu, Wu-Ming Kong , Yuan Liu , Wei-Xiong Chen , Xiao-Hong Liao. Silencing of MAP4K4 by short hairpin RNA suppresses proliferation, induces G1 cell cycle arrest and induces apoptosis in gastric cancer cells. *Mol Med Rep* 2016; 13: 41-48.

40 Joseph C Loftus ZY, Jean Kloss, Harshil Dhruv, Nhan L Tran, Daniel L Riggs. A Novel Interaction between Pyk2 and MAP4K4 Is integrated with glioma cell migration. *J Signal Transduct* 2013: 956580.

41 Collins CS HJ, Sapinoso L, Zhou Y, Liu Z, Micklash K, Schultz PG, Hampton GM A small interfering RNA screen for modulators of tumor cell motility identifies MAP4K4 as a promigratory kinase . *Proc Natl Acad Sci* 2006; 103: 3775–3780.

42 Su-Xia Han QZ, Jin-Lu Ma, Jing Zhao, Chen Huang, Xi Jia, Dan Zhang. Lowered HGK expression inhibits cell invasion and adhesion in hepatocellular carcinoma cell line HepG2. *World J Gastroenterol* 2010; 16: 4541-4548.

43 Philip Vitorino SY, Ailey Crow , Jesse Bakke , Tanya Smyczek , Kristina West , Erin McNamara , Jeffrey Eastham-Anderson , Stephen Gould , Seth F Harris , Chudi Ndubaku , Weilan Ye. MAP4K4 regulates integrin-FERM binding to control endothelial cell motility. *Nature* 2015; 519: 425-430.

Figures

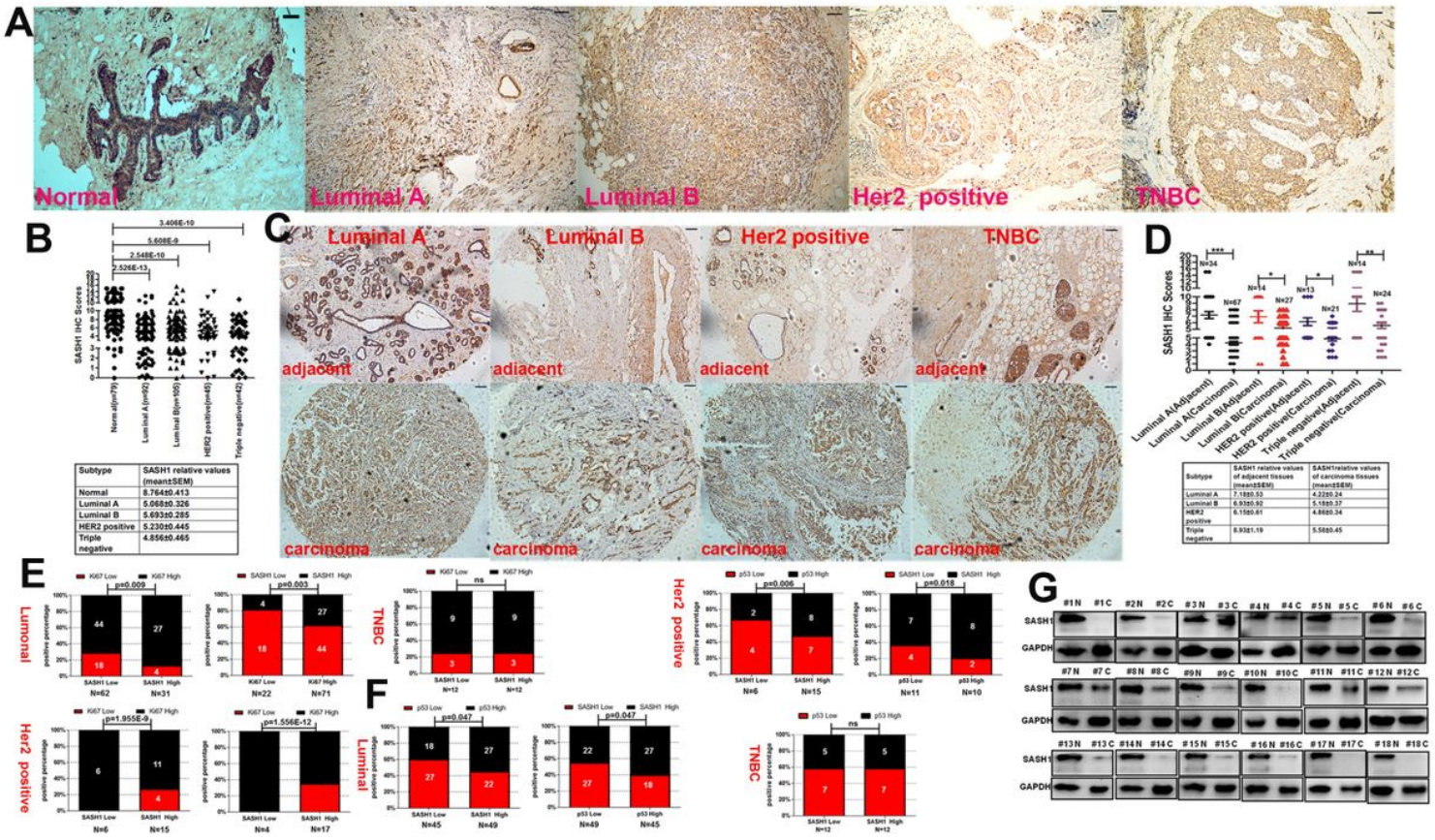

Figure 1

SASH1 expression is decreased in different subtypes of breast carcinoma tissues. A IHC determination of SASH1 expression levels of different breast cancer subtypes and normal breast tissues. A representative image of SASH1 IHC staining in tissues of different breast cancer subtypes and normal breast tissues is showed, respectively. bar:10μm and Magnification: 10x. B The IHC scores of SASH1 of four cancer subtypes and normal breast cancer were analyzed statistically and statistical analyses indicated that SASH1 expression was downregulated in four subtype breast cancers compared with that of normal breast cancer. C IHC staining of an array with 139 human breast carcinoma tissues (bottom panels) and matched adjacent tissues (upper panels). A representative image of SASH1 IHC staining in breast cancer subtypes and adjacent tissues. bar: 10μm and Magnification: 10x. D Statistical analysis of SASH1 IHC scores in tissue arrays showed that SASH1 expression was decreased in different of breast carcinoma subtypes as compared with adjacent breast tissues*P<0.05, ** P <0.01, *** P <0.001. E Statistical analyses of IHC scores of SASH1 and Ki67 in tissue arrays showed that SASH1 expression was negatively associated with that of Ki67 in subtypes of luminal and Her2 positive. However, SASH1 expression was not associated with that of Ki67 in TNBC subtype. F Statistical analyses of IHC scores of SASH1 and 53 tissue arrays showed that SASH1 expression was positively associated with that of p53 in subtypes of luminal and Her2 positive. However, SASH1 expression was not associated with that of p53 in TNBC subtype. G Immunoblotting analyses identified that SASH1expression was decreased in most breast carcinoma subtypes compared with normal breast tissues. N = benign tissues. C = cancer tissues.

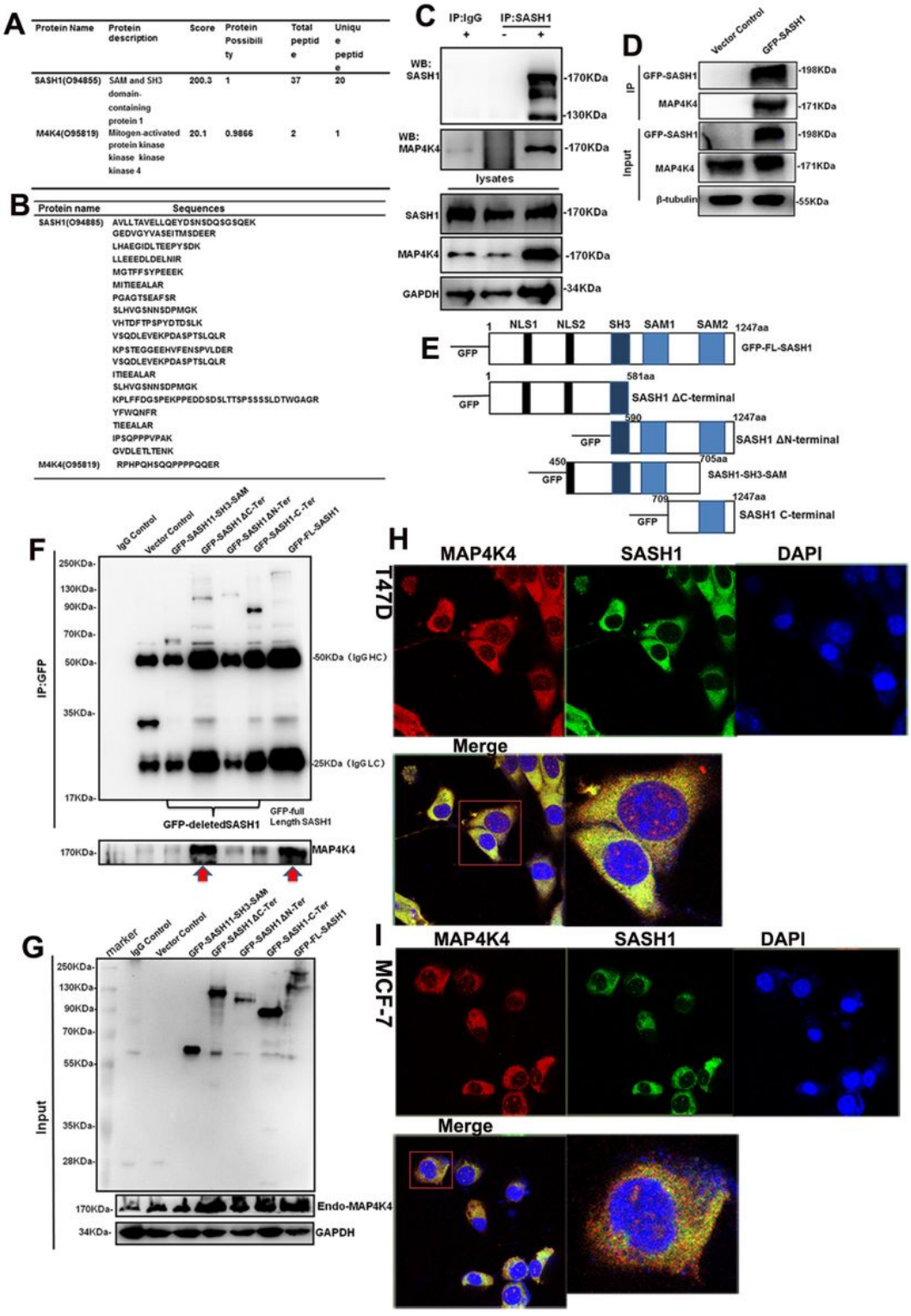

Figure 2

SASH1 binds to MAP4K4 . A Proteins that probably bind with SASH1 in stable SK-BR-3 cells were identified by LC/LC MS analysis. B The peptide sequences of the SASH1 complex identified by LC-MS/MS and bioinformatics analyses. C The association between endogenous SASH1 and endogenous MAP4K4 was identified by IP-WB in SK-BR-3 cells. D The association between exogenous SASH1 and endogenous MAP4K4 in SK-BR-3 cells was identified by IP-WB. E Schematic viewing of SASH1 mutants. F and G The

N-terminal domain (aa 1-581) of SASH1 binds to MAP4K4. H The co-localization between SASH1 and MAP4K4. Immunofluorescence(IF) laser confocal microscopy was used to observe the expression of endogenous SASH1 and endogenous MAP4K4 in T47D and MCF-7 cells after crawled on the slides. T47D and MCF-7 cells were stained with SASH1 antibody (green) and MAP4K4 antibody (red) with immunofluorescence and photographed by confocal microscope.

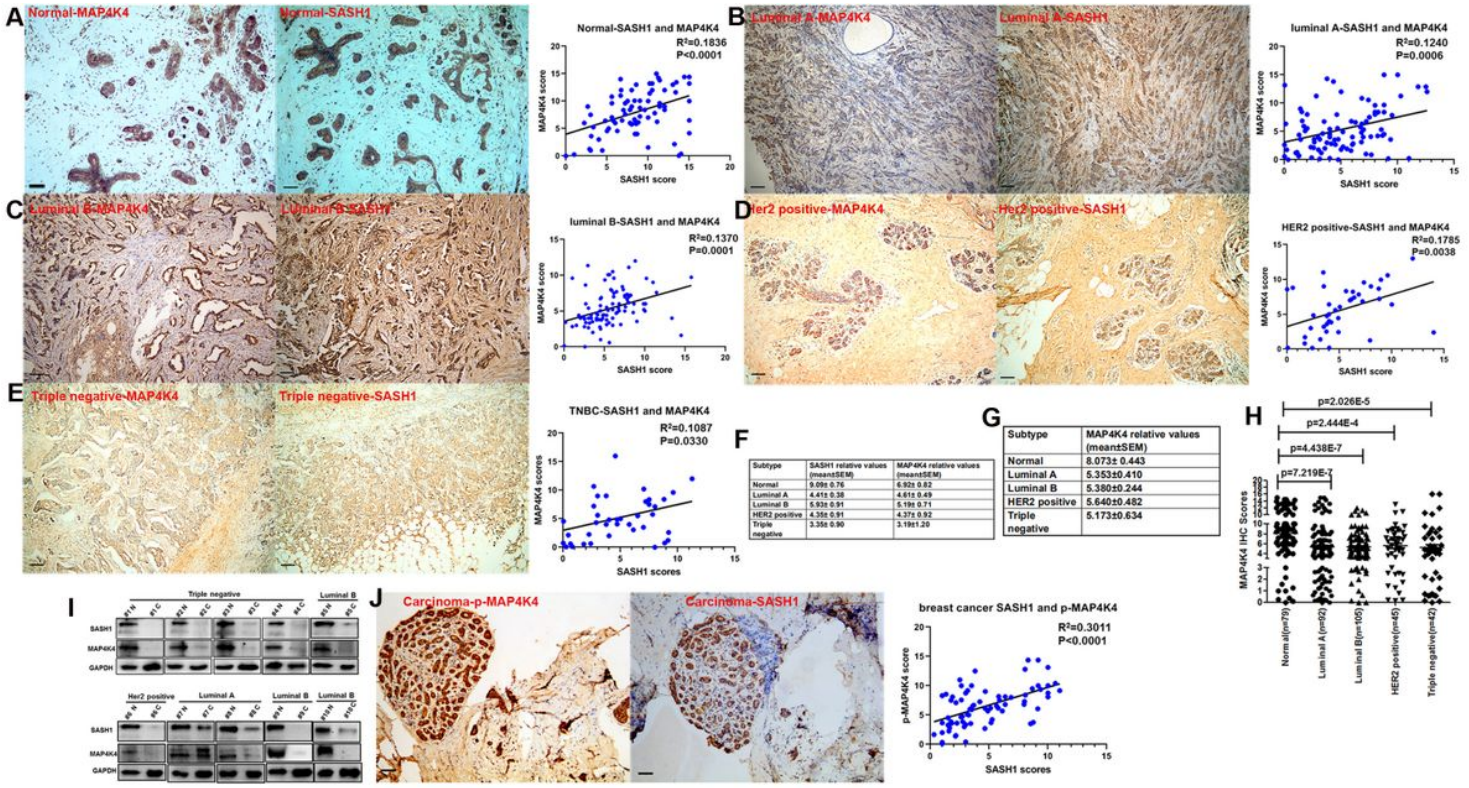

Figure 3

SASH1 expression is positively correlated with MAP4K4 expression in the breast cancer tissues and normal breast tissues. A A representative image of IHC staining of SASH1 and MAP4K4 in 79 benign breast tissues. Statistical analysis of SASH1 and MAP4K4 scores revealed that SASH1 expression was correlated with MAP4K4 (right panel). B, C, D and E A representative image of IHC staining of SASH1 and MAP4K4 in the breast cancer tissues of 92 luminal A,105 luminal B,45 Her2 positive and 42 TNBC subtype. In luminal A, luminal B and Her2 positive subtype, SASH1 was significantly associated with MAP4K4. F The statistical analyses data of IHC scores of SASH1 and MAP4K4 in normal breast tissues and four subtype breast cancer. G and H IHC staining of MAP4K4 expression and statistical analyses indicated that MAP4K4 was downregulated in four subtypes of breast cancer compared with benign breast tissues. I Immunoblotting analysis showed that the expression of SASH1 and MAP4K4 was decreased in most different breast carcinoma subtypes compared with benign breast tissues. J A representative image of IHC staining of SASH1 and phospho-MAP4K4 in 75 breast cancer tissues. Statistical analysis revealed that SASH1 expression was significantly correlated with phospho-MAP4K4 levels in 75 breast cancer tissues. bar:10μm. Magnification: 10x.

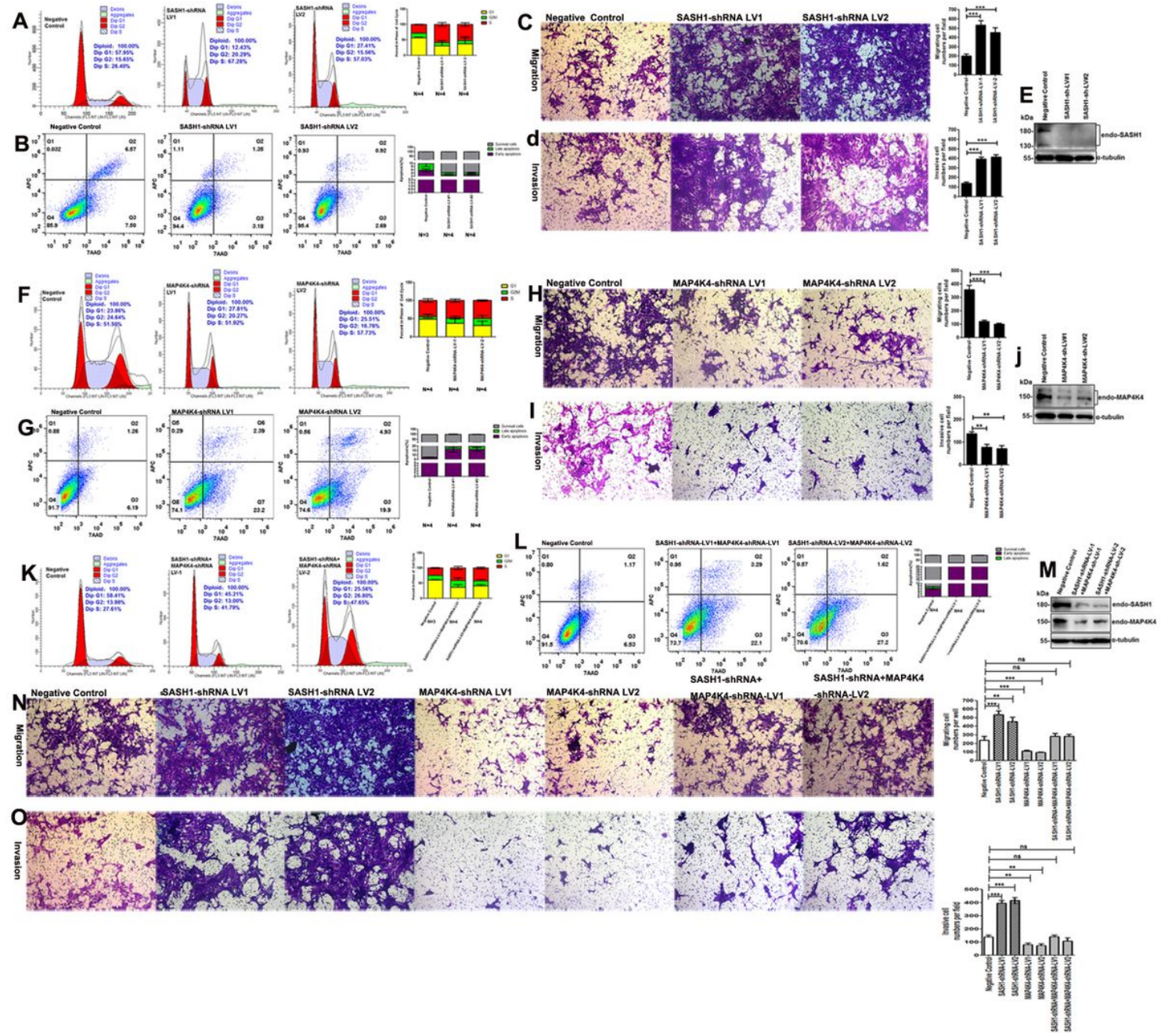

Figure 4

MAP4K4 and SASH1 coordinate and regulate the cell proliferation, cell migration and invasion of ER positive breast cancer cells. A SASH1 silencing by shRNA induced an increase in the proportion pf S-phase cells in T47D stable cells infected with SASH1-shRNA lentivirus. T47D stable cells were starved for 72hr and the cell cycle distribution of T47D cells was analyzed . B SASH1 silencing inhibited the apoptosis of T47D cells. Flow cytometry assays indicated that SASH1 silencing caused a significant increase in the proportion of apoptotic cells. C, D and E Migration and invasion of T47D cells were induced by SASH1 silencing. The transwell migration assay and the transwell invasion assay were performed to analyze after T47D stable cells being starved for 72hr. The migrating and invasive cells were counted and analyzed statistically. ***p<0.001. The silencing efficiency of SASH1- shRNAs was

examined by western blot. F MAP4K4 knockdown caused a G2/M-phase arrest in T47D stable cells. T47D stable cells were starved for 72hr and subjected to flow cytometry analysis of the cell cycle. G MAP4K4 deletion significantly increased the proportion of apoptotic cells in T47D stable cells. H, I and J The transwell migration assay and the transwell invasion assay indicated that MAP4K4 depletion decreased the migration and invasion ability of T47D cells. **p<0.01, ***p<0.001. The silencing efficiency of MAP4K4 shRNAs was examined by western blot. K The increase in S-phase cells induced by SASH1 silencing in T47D stable cells was abolished by MAP4K4 silencing and the subsequent G2/M-phase arrest was observed. L and M The decreased proportion of apoptotic cells induced by SASH1 silencing in T47D stable cells was abolished by MAP4K4 silencing and the enhanced proportion of apoptotic cells was observed. The silencing efficiency of shRNAs of SASH1 and MAP4K4 was detected by western blot. N and O The enhanced ability of migration and invasion of T47D cells induced by SASH1 knockdown was impaired by MAP4K4 depletion. **p<0.01,***p<0.001,ns no significance. These data were representative results of at least 3 repeated experiments with similar trends.

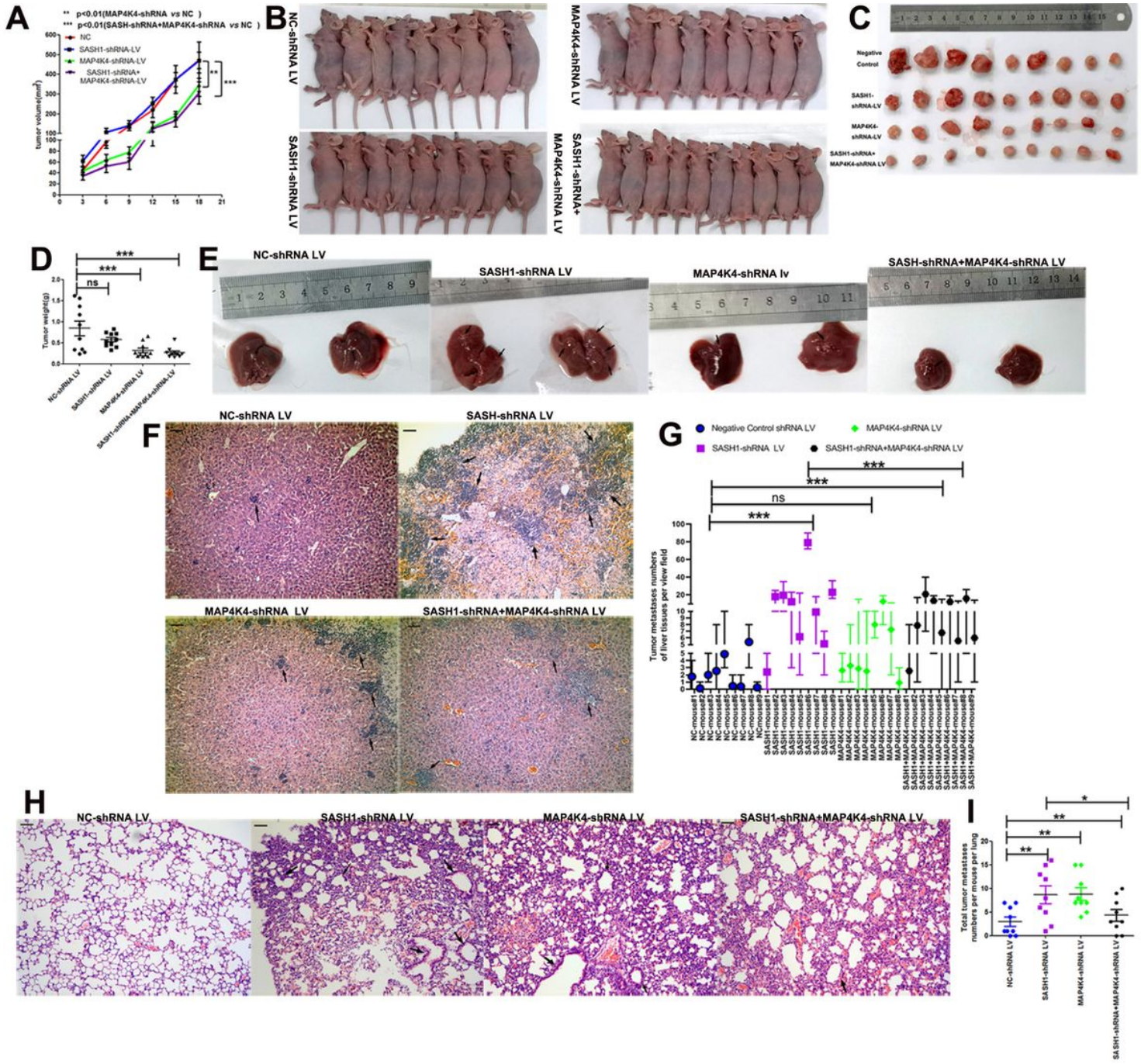

Figure 5

SASH1 deletion-induced- cell proliferation and metastasis were impaired by MAP4K4 silencing in vivo. A MAP4K4 silencing and co-silencing of SASH1 and MAP4K4 blocked the xenograft tumor growth of T47D cells. T47D cells stably infected with SASH1- and/or MAP4K4-shRNA lentivirus were injected subcutaneously into the left side fossa axillaris of BALB/c female nude mice . The nude mice bearing negative control-shRNA, SASH1- and/or MAP4K4-shRNA were randomly assigned to four groups with 10-13 mice in each group. The tumor sizes of nude mice were monitored over a period of 18 days. B, C and D MAP4K4 knockdown and co-knockdown of SASH1 and MAP4K4 inhibited the proliferation of T47D cells-xenograft tumors. After the monitoring and observation for three weeks, animals were sacrificed and tumors were excised. Tumor diameters and tumor weight were measured and tumor volumes were

calculated. Values are mean ± SD. ***p<0.001. E Liver tissues were photographed and the black arrows indicate the liver metastatic lesions. F More live metastatic lesions were observed in the nude mice bearing SASH1 knockdown- xenograft tumors. However, MAP4K4 knockdown impaired the inducement of more live metastatic lesions by SASH1 silencing in the nude mice with co-silencing SASH1 and MAP4K4-xenograft tumors. Liver tissues were photographed, fixed, and stained with hematoxylin and eosin (H&E). The numbers of metastatic lesions of each mouse were counted and compared statistical analyses. ***p<0.001. G Increased pulmonary metastatic lesions were observed in the nude mice bearing SASH1 deletion-xenograft tumors. However, MAP4K4 silencing abolished the inducement of more pulmonary metastatic lesions by SASH1 silencing in the nude mice with co-silencing SASH1 and MAP4K4-xenograft tumors. Lung tissues were photographed, fixed and subjected to HE staining. The total numbers of pulmonary metastatic lesions in one lung tissues of each mouse were counted and analyzed statistically. *p<0.05, **p<0.01. bar:10cm.

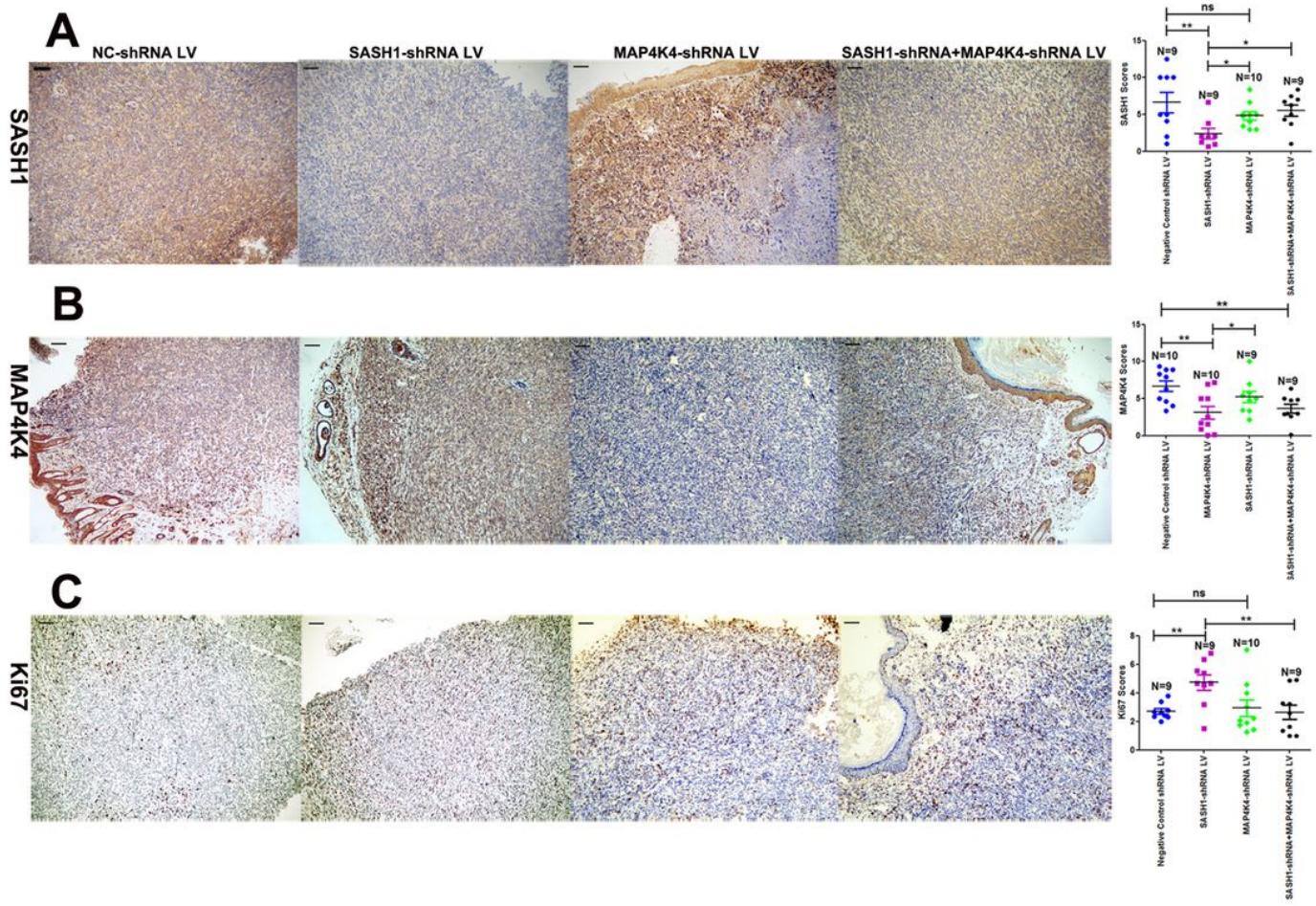

Figure 6

The parameter index of cell proliferation induced by SASH1 deletion were impaired by MAP4K4 silencing in vivo. A MAP4K4 deletion in vivo reversed the SASH1 downregulation induced by SASH1 silencing in the T47D cells- xenograft tumors bearing SASH1 and MAP4K4-co-silencing , and MAP4K4 silencing upregulated SASH1 expression in the xenograft tumors stable expressing MAP4K4-shRNA lentivirus. The SASH1 expression of the xenograft tumors containing SASH1 and/or MAP4K4 -shRNA lentivirus as well

as the negative control lentivirus were analyzed by IHC. The SASH1 expression were scored according to the positive areas and positive intensity of SASH1.The SASH1 scores were analyzed using one-way ANOVA and the cartograms were plotted. The mice numbers in each group were indicated in the cartograms and the SASH1 scores between the xenograft tumors expressing negative control-shRNA lentivirus(NC-shRNA LV) and SASH1-shRNA LV, those expressing SASH1-shRNA LV and MAP4K4- shRNA LV, those expressing SASH1-shRNA LV and SASH1-shRNA+ MAP4K4- shRNA LV and those NC-shRNA LV and MAP4K4-shRNA LV were compared. **p<0.01,*p<0.05,ns no significance. B SASH1 silencing may promote MAP4K4 expression in the xenograft tumors containing SASH1-shRNA lentivirus. **p<0.01, *p<0.05. C SASH1 silencing upregulated Ki67 expression and increased Ki67-positive cells in the xenograft tumors containing SASH1-shRNA lentivirus. MAP4K4 knockdown impaired the inducement of Ki67 expression and increased Ki67-positive cells by SASH1 silencing in the xenograft tumors containing the lentivirus of SASH1-shRNA and MAP4K4-MAP4K4. bar: 10μm.

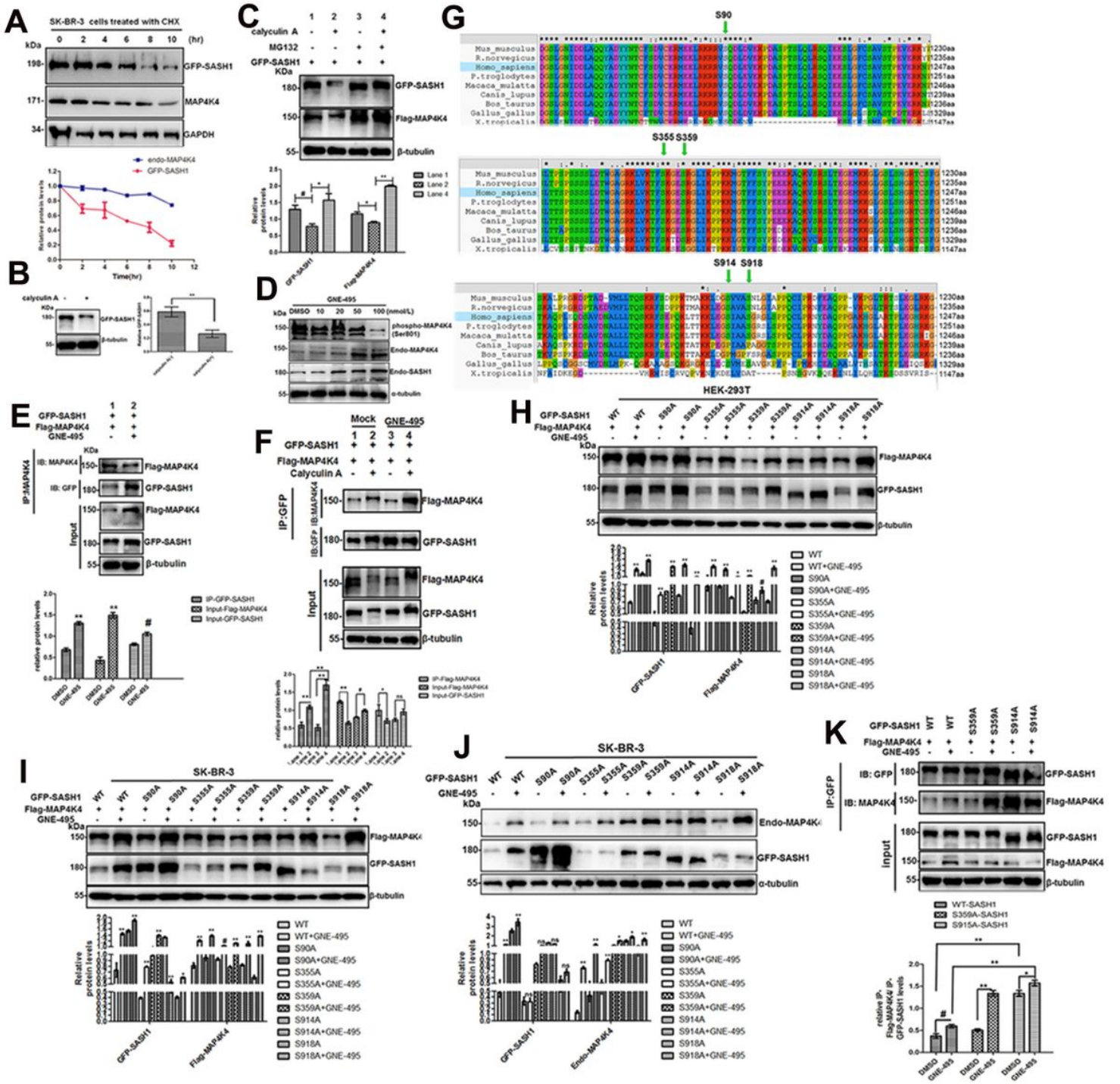

Figure 7

SASH1, a novel protein kinase, is phosphorylated by MAP4K4 A SASH1 was a very unstable protein. Exogenous SASH1 and endogenous MAP4K4 are both degraded upon CHX treatment in SK-BR-3 transfected cells. B Calyculin A decreased SASH1 protein levels in SK-BR-3 cells. ** P <0.01. C MG132 not only blocked calyculin A-induced SASH1 degradation but also calyculin A-induced MAP4K4 degradation. **P<0.001,*P<0.01□#P<0.05 . D Phosphorylation levels of endogenous MAP4K4 were inhibited by 100nM GNE-495. SK-BR-3 cells were treated with different doses of GNE-495 for 24hr to test the GNE-495 efficiency to suppress the MAP4K4 phosphorylation levels. The phospho-MAP4K4, endogenous MAP4K4

and endogenous SASH1 protein levels in SK-BR-3 cells were assessed by western blot. E GNE-495 not only upregulated SASH1 and MAP4K4 expression but induced the binding of SASH1 to MAP4K4. ** P <0.001, # P <0.01. F GNE-495(100 nM) efficiently blocked calyculin A-induced phosphorylation and degradation of exogenous SASH1 and MAP4K4, and promoted binding of MAP4K4 to SASH1. ** P <0.001, # P <0.01, * P <0.05. G Ser90, Ser355, Ser359, Ser914 , and Ser918 of SASH1, identified by LC-MS/MS analyses are highly conserved , as indicated by Clustal X2 software. H, I and J S914A mutation of SASH1 caused the forward shift of SASH1 and countered the upregulation of exogenous or endogenous SASH1 induced by MAP4K4 in HEK-293T and SK-BR-3 cells treated with GNE-495 as determined by western blot . **P<0.001,*P<0.01#P<0.05 ,the cells transfected with wild type or mutated SASH1 vectors and treated with GNE-495 vs those transfected with wild type or mutated SASH1 vectors only. K S914A mutation of SASH1 significantly promoted the binding of SASH1 to MAP4K4 . GNE-495 increased not only the binding of wild type SASH1 to MAP4K4 but also of SASH1 mutants. The amount of Flag-MAP4K4 in the immunoprecipitates was quantified and normalized to GFP-SASH1. ** P <0.001, # P <0.01* P <0.05. Data are represented as the mean ± SD; Western blots shown are representative images of at least 3 independent experiments.

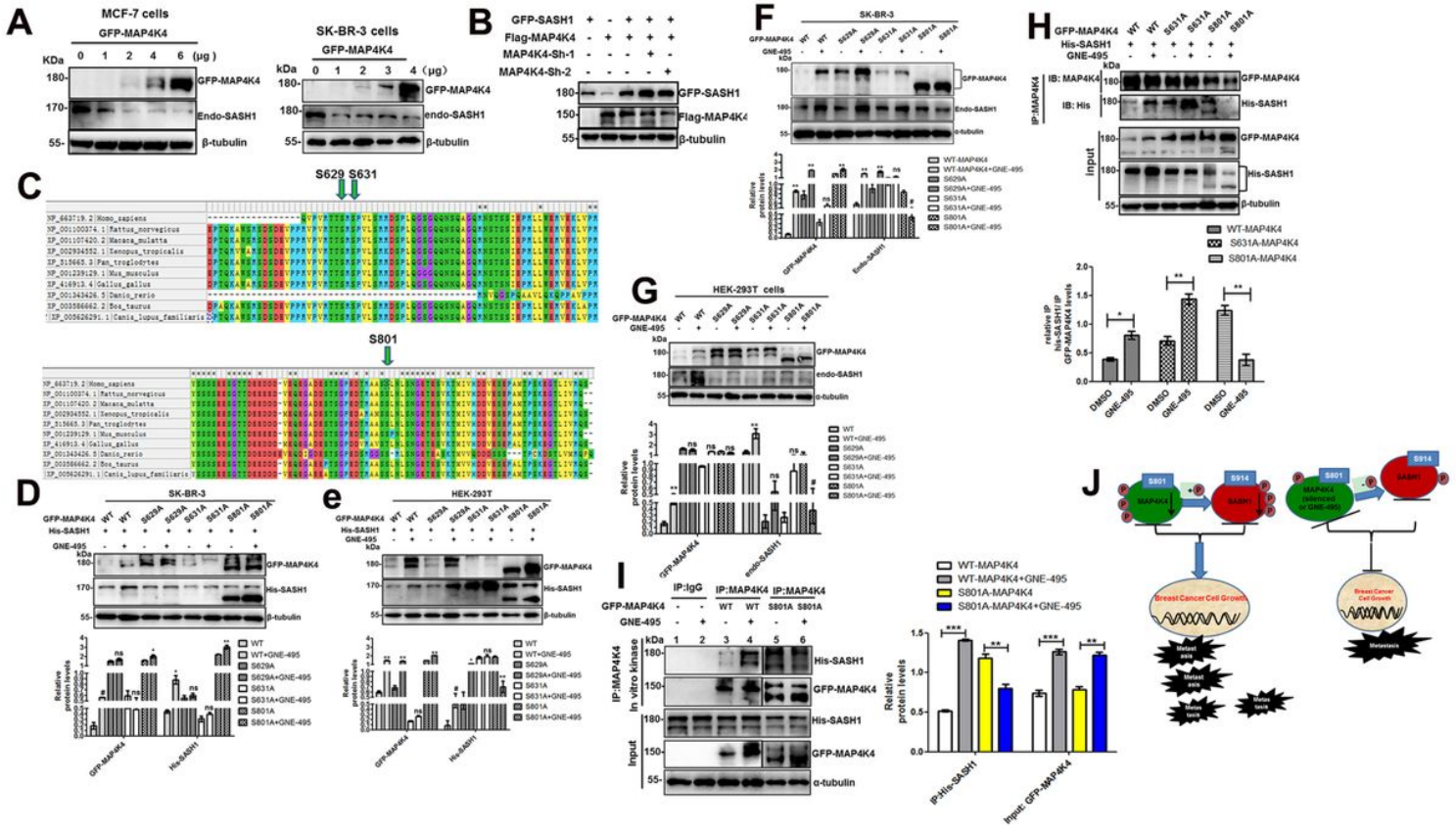

Figure 8

MAP4K4 phosphorylates SASH1 at Ser801 site. A Downregulation of endogenous SASH1 was induced by increasing doses of exogenous MAP4K4. Increasing doses of GFP-MAP4K4 were introduced into MCF-7 and SK-BR-3 cells respectively. At 36 hr post-transfection, cells were lysed and subjected to western blot. B MAP4K4 knock-down upregulated exogenous SASH1 expression. SK-BR-3 cells were transfected with

exogenous SASH1(GFP-SASH1) and exogenous MAP4K4(Flag-MAP4K4) and silenced with MAP4K4-shRNA. After transfection for 48hr, transfected cells were subjected to western blot. C The MAP4K4 phosphorylation sites Ser629, Ser631 and Ser801 were highly conserved. The conservation of serine residues of MAP4K4 was analyzed by MEGA-X software. D and E Ser801 of MAP4K4 is the key phosphorylation site of SASH1 and its phosphorylation induced forward shift of the MAP4K4 protein bands. S801A in MAP4K4 abolished the upregulation of exogenous SASH1 induced by mutated MAP4K4 when transfected HEK-293T cells were treated with GNE-495. GFP-MAP4K4 with wild type and MAP4K4 mutants, and his-SASH1 were transfect into SK-BR-3 and HEK-293T cells. After transfection for 40hr, cells were treated with 100 nM GNE-495 for 24hr and subjected to immunoblot. F and G S801A mutation in MAP4K4 impaired the upregulation of endogenous SASH1 induced by GNE-495. SK-BR-3 and HEK-293T cells were transfected with GFP-MAP4K4 with wild type and MAP4K4 mutants. At 24hr after transfection, the transfected cells were treated with 100 nM GNE-495 for 24hr and the expression of exogenous MAP4K4 and endogenous SASH1 were assessed by immunoblotting. H The S801A mutation in MAP4K4 abolished the increased bindings of MAP4K4 to SASH1 induced by GNE-495. Exogenous wild type MAP4K4 and MAP4K4 mutants as well as His-SASH1 were introduced into HEK-293T cells. After transfection for 40hr, cells were treated with GNE-495 for 24hr, lysed and used for immunoprecipitation with anti-MAP4K4 antibody. The associated GFP-SASH1 was analyzed. #P<0.05, *P<0.01, **P<0.001, ns no significance. (I) Kinase activity of SASH1 and MAP4K4 was inhibited by GNE-495 treatment. HEK-293T cells were transfected with wild type MAP4K4 and S801A- MAP4K4 ,and then treated with GNE-495 for 24hr. Meanwhile HEK-293T cells were also introduced with His-SASH1. Immunoprecipitated MAP4K4 was subjected to an in vitro kinase assay using His-SASH1 as a substrate. The phosphorylation changes of SASH1 and MAP4K4 was only reflected by their expression changes after GNE-495 treatment. ***P<0.001. Data are represented as the mean ± SD; Blots shown are representative images of 3 independent experiments. J A working model illustrating regulation between SASH1 and MAP4K4. MAP4K4 phosphorylates SASH1 and induces subsequent degradation of phosphorylation, which will eventually promote tumorigenesis and metastasis of breast cancer. Deleted MAP4K4 by shRNA silencing or MAP4K4 treated with GNE-495 will affect the phosphorylation of MAP4K4 to SASH1 to induce SASH1 upregulation, which will eventually block tumorigenesis and metastasis of hormone-dependent breast cancer.

Supplementary Files

This is a list of supplementary files associated with this preprint. Click to download.

- 20201009FigureS1.jpg
- 20201009FigureS2.jpg
- 20201009SupplementaryFigure3.jpg
- 20201009FigureS4.jpg
- 20201028FigureS5.tif

- 20201019TableS1.docx
- 20201019TableS2.docx
- 20201019SupplementaryMaterialsandMethods.docx